

Context-aware Feature Generation for Zero-shot Semantic Segmentation

Zhangxuan Gu Siyuan Zhou Li Niu*
 MoE Key Lab of Artificial Intelligence, MoE Key Lab of Artificial Intelligence, MoE Key Lab of Artificial Intelligence,
 Shanghai Jiao Tong University Shanghai Jiao Tong University Shanghai Jiao Tong University
 zhangxgu@126.com ssluvble@sjtu.edu.cn ustcnewly@sjtu.edu.cn

Zihan Zhao Liqing Zhang*
 MoE Key Lab of Artificial Intelligence, MoE Key Lab of Artificial Intelligence,
 Shanghai Jiao Tong University Shanghai Jiao Tong University
 john745111625@gmail.com zhang-lq@cs.sjtu.edu.cn

ABSTRACT

Existing semantic segmentation models heavily rely on dense pixel-wise annotations. To reduce the annotation pressure, we focus on a challenging task named zero-shot semantic segmentation, which aims to segment unseen objects with zero annotations. This task can be accomplished by transferring knowledge across categories via semantic word embeddings. In this paper, we propose a novel context-aware feature generation method for zero-shot segmentation named CaGNet. In particular, with the observation that a pixel-wise feature highly depends on its contextual information, we insert a contextual module in a segmentation network to capture the pixel-wise contextual information, which guides the process of generating more diverse and context-aware features from semantic word embeddings. Our method achieves state-of-the-art results on three benchmark datasets for zero-shot segmentation. *Codes are available at: <https://github.com/bcmi/CaGNet-Zero-Shot-Semantic-Segmentation>*

CCS CONCEPTS

• Computing methodologies → Image segmentation.

KEYWORDS

zero-shot semantic segmentation, contextual information, feature generation

ACM Reference Format:

Zhangxuan Gu, Siyuan Zhou, Li Niu*, Zihan Zhao, and Liqing Zhang*. 2020. Context-aware Feature Generation for Zero-shot Semantic Segmentation. In *Proceedings of the 28th ACM International Conference on Multimedia (MM '20)*, October 12–16, 2020, Seattle, WA, USA. ACM, New York, NY, USA, 9 pages. <https://doi.org/10.1145/3394171.3413593>

*Corresponding authors.

Permission to make digital or hard copies of all or part of this work for personal or classroom use is granted without fee provided that copies are not made or distributed for profit or commercial advantage and that copies bear this notice and the full citation on the first page. Copyrights for components of this work owned by others than ACM must be honored. Abstracting with credit is permitted. To copy otherwise, or republish, to post on servers or to redistribute to lists, requires prior specific permission and/or a fee. Request permissions from permissions@acm.org.

MM '20, October 12–16, 2020, Seattle, WA, USA

© 2020 Association for Computing Machinery.

ACM ISBN 978-1-4503-7988-5/20/10...\$15.00

<https://doi.org/10.1145/3394171.3413593>

1 INTRODUCTION

Semantic segmentation, aiming at classifying each pixel in one image, heavily relies on the dense pixel-wise annotations [5, 25, 26, 38, 50, 53]. To reduce the annotation pressure, leveraging weak annotations like image-level [34, 35, 47], box-level [18, 36], or scribble-level [24] annotations for semantic segmentation recently gained the interest of researchers. In this work, we focus on a more challenging task named zero-shot semantic segmentation [3], which further relieves the burden of human annotation. Similar to zero-shot learning [21], we divide all categories into seen and unseen categories. The training images only have pixel-wise annotation for seen categories, while both seen and unseen objects may appear in test images. Thus, we need to bridge the gap between seen and unseen categories via category-level semantic information, enabling the model to segment unseen objects in the testing stage.

Transferring knowledge from seen categories to unseen categories is not a new idea and has been actively studied by zero-shot learning (ZSL) [2, 10, 21, 45]. Most ZSL methods tend to learn the mapping between visual features and semantic word embeddings or synthesize visual features for unseen categories.

To the best of our knowledge, there are quite few works on zero-shot semantic segmentation [3, 17, 43, 49], in which only SPNet [43] and ZS3Net [3] can segment an image with multiple categories. SPNet extends a segmentation network by projecting visual features to semantic word embeddings. Since the training images only contain labeled pixels of seen categories, the prediction will be biased towards seen categories in the testing stage. Hence, they deduct the prediction scores of seen categories by a calibration factor during testing. However, the bias issue is still severe after using calibration. Inspired by feature generation methods for zero-shot classification [7, 44], ZS3Net learns to generate pixel-wise features from semantic word embeddings. The generator is trained with seen categories and able to produce features for unseen categories, which are then used to finetune the last 1×1 convolutional (conv) layer in the segmentation network. Moreover, they extend ZS3Net to ZS3Net (GC) by using Graph Convolutional Network (GCN) [19] to capture spatial relationships among different objects. However, it still has two drawbacks: 1) ZS3Net simply appends a random noise to one semantic word embedding to generate diverse features. However, the generator often ignores the random noise and can only produce limited diversity for each category-level semantic word

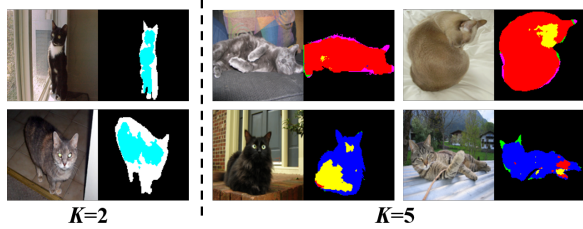


Figure 1: The pixel-wise visual features of category “cat” are grouped into K clusters with each color representing one cluster in Pascal-Context. The left (*resp.*, right) subfigure shows the visualization results when $K = 2$ (*resp.*, $K = 5$).

embedding, known as mode collapse problem [42, 51]; 2) Although ZS3Net (GC) utilizes relational graphs to encode spatial object arrangement, the contextual cues it considers are object-level and only limited to spatial object arrangement. Moreover, the relational graphs containing unseen categories are usually inaccessible when generating unseen features.

In this paper, we follow the research line of feature generation for zero-shot segmentation and propose a Contextual-aware feature Generation model, CaGNet, by considering pixel-wise contextual information when generating features.

The contextual information of a pixel means the information inferred from its surrounding pixels (e.g., its location in the object, the posture of the object it belongs to, background objects), which is not limited to spatial object arrangement considered in [3]. Intuitively, the pixel-wise feature vectors in deep layers highly depend on their contextual information. To corroborate this point, we obtain the output features of the ASPP module in Deeplabv2 [5] for category “cat” on Pascal-Context [31], and group those pixel-wise features into K clusters by K-means. Based on Figure 1, we observe that pixel-wise features are affected by their contextual information in an interlaced and complicated way. When $K = 2$, the features from the interior (*resp.*, exterior) of the cat are grouped together. When $K = 5$, we provide examples in which pixel-wise features are affected by adjacent or distant background objects. For example, the red (*resp.*, blue) cluster is likely to be influenced by the cushion (*resp.*, green plant) as shown in the top (*resp.*, bottom) row. These observations motivate us to generate context-aware features with the guidance of pixel-wise contextual information.

Unlike the feature generator in ZS3Net, which takes semantic word embedding and random noise as input to generate pixel-wise fake feature, we feed semantic word embedding and pixel-wise contextual latent code into our generator. The contextual latent code is obtained from our proposed Contextual Module (CM). Our CM takes the output of the segmentation backbone as input and outputs pixel-wise real feature and corresponding pixel-wise contextual latent code for all pixels. In our CM, we also design a context selector to adaptively weight different scales of contextual information for different pixels. Since adequate contextual information is passed to the generator to resolve the ambiguity of feature generation, we expect that the pixel-wise contextual latent code together with semantic word embedding is able to reconstruct the pixel-wise real feature. In other words, we build the one-to-one correspondence

(bijection) between input pixel-wise contextual latent code and output pixel-wise feature. It has been proved in [52] that the bijection between input latent code and output could mitigate the mode collapse problem, so our model can generate more diverse features from one semantic word embedding by varying the contextual latent code. We enforce the contextual latent code to follow unit Gaussian distribution to get various contextual latent codes via randomly sampling. Therefore, the segmentation network and our feature generation network are linked by contextual module and classifier.

In summary, compared with ZS3Net, CaGNet can produce more diverse and context-aware features. Compared with its extension ZS3Net (GC), our method has two advantages: 1) we leverage more informative pixel-wise contextual information instead of object-level contextual information; 2) we encode contextual information into latent code, which supports stochastic sampling, so we do not require explicit contextual information of unseen categories (e.g., relational graph) when generating unseen features. Our main contributions are:

- We design a feature generator guided by pixel-wise contextual information, to obtain diverse and context-aware features for zero-shot semantic segmentation.
- Two minor contributions are: 1) unification of segmentation network and feature generation network; 2) contextual module with a novel context selector.
- Extensive experiments on Pascal-Context, COCO-stuff, and Pascal-VOC demonstrate the effectiveness of our method.

2 RELATED WORKS

Semantic Segmentation: State-of-the-art semantic segmentation models [5, 25, 26, 38, 50, 53] are typically extending Fully Convolutional Network (FCN) [26] framework with larger receptive field and more efficient encoder-decoder structure. Based on the idea to expand receptive field, PSPNet[50] and Deeplab[5] design specialized pooling layers for fusing the contextual information from feature maps of different scales. Other methods like U-Net [38] and RefineNet [25] focus on designing more efficient network architectures to better combine low-level and high-level features.

One important characteristic of semantic segmentation is the usage of contextual information since the category predictions of target objects are often influenced by nearby objects or background scenes. Thus, many works [5, 48] tend to explore contexts of different receptive fields with dilated convolutional layers, which also motivates us to incorporate contexts into feature generation. However, those models still require annotations of all categories during training, and thus cannot be applied to the zero-shot segmentation task. In contrast, we successfully combine segmentation network with feature generator for zero-shot semantic segmentation.

Zero-shot Learning: Zero-shot learning (ZSL) was first introduced by [20], in which training data are from seen categories, but test data may come from unseen categories. Knowledge is transferred from seen categories to unseen via category-level semantic embeddings. Many ZSL methods [1, 8, 9, 11, 27, 32, 33, 37, 46] attempted to learn a mapping between feature space and semantic embedding space.

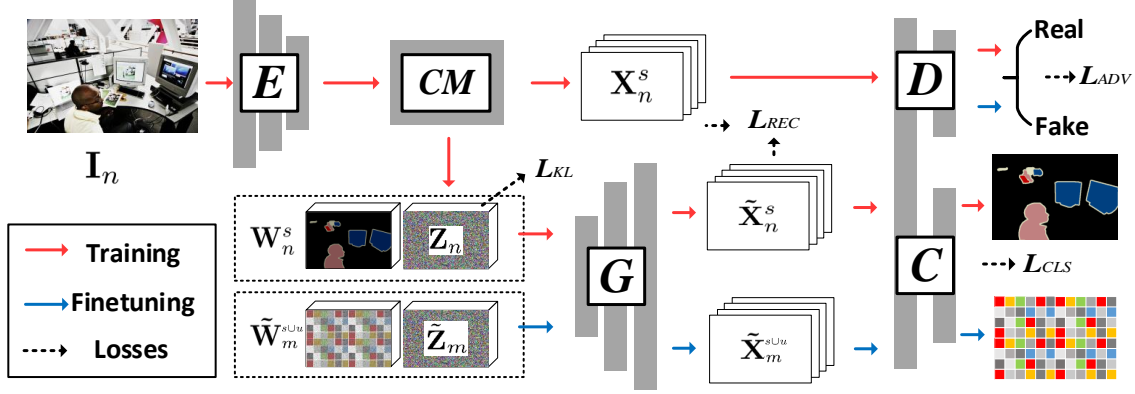


Figure 2: Overview of our CaGNet. Our model contains segmentation backbone E , Contextual Module CM , feature generator G , discriminator D , and classifier C . W , Z , and X represent semantic word embedding map, contextual latent code map, and feature map respectively (see Section 3.2 and 3.3 for detailed definition). Optimization steps are separated into training step and finetuning step indicated by two different colors (see Section 3.4).

Recently, a popular approach of zero-shot classification is generating synthesized features for unseen categories. For example, the method in [44] first generated features using word embeddings and random vectors, which was further improved by later works [7, 22, 28, 40, 45]. These zero-shot classification methods generated image features without involving contextual information. In contrast, due to the uniqueness of semantic segmentation, we utilize pixel-wise contextual information to generate pixel-wise features. **Zero-shot Semantic Segmentation:** The term zero-shot semantic segmentation appeared in prior works [3, 17, 43, 49], in which only SPNet [43] and ZS3Net [3] focused on multi-category semantic segmentation. SPNet achieves knowledge transfer between seen and unseen categories via semantic projection layer and calibration method, while ZS3Net aims to generate pixel-wise features to finetune the classifier, which is biased to the seen categories. Our method is inspired by ZS3Net, but different from their method in mainly two ways: 1) we unify the segmentation network and feature generator; 2) we leverage pixel-wise contextual information to guide feature generation.

3 METHODOLOGY

For ease of representation, we denote the set of seen (*resp.*, unseen) categories as C^s (*resp.*, C^u) and $C^s \cap C^u = \emptyset$. In the zero-shot segmentation task, the training set only contains pixel-wise annotations of C^s , while the trained model is supposed to segment objects of $C^s \cup C^u$ at test time. As mentioned in Section 1, the bridge between seen and unseen categories is the category-level semantic word embeddings $\{\tilde{w}_c | c \in C^s \cup C^u\}$, in which $\tilde{w}_c \in \mathcal{R}^d$ is the semantic word embedding of category c .

3.1 Overview

Our method, CaGNet, can be applied to an arbitrary segmentation network. We start from Deeplabv2 [5], which has shown remarkable performance in semantic segmentation. Any segmentation network

like Deeplabv2 can be separated into two parts: backbone E and classifier C (e.g., one or two 1×1 conv layers). Given an input image, the backbone outputs its real feature map, which is passed to the classifier to get the segmentation results.

To enable the segmentation network to segment unseen objects, we aim to learn a generator G to generate features for unseen categories. As shown in Figure 2, G takes the semantic word embedding map and the latent code map as input to output fake features. Then, discriminator D and classifier C , with a shared 1×1 conv layer, take real/fake features to output discrimination and segmentation results respectively. Note that our classifier C is shared by the feature generation network and the segmentation network. To help the generator G produce more diverse and context-aware features, we insert a Contextual Module (CM) after the backbone E of segmentation network to obtain contextual information, which is encoded into the latent code as the guidance of G . Therefore, we unify the segmentation network $\{E, CM, C\}$ and the feature generation network $\{CM, G, D, C\}$, which are linked by Contextual Module CM and classifier C . Next, we will detail our CM in Section 3.2 and feature generator in Section 3.3. For ease of description, we use capital letter in bold (e.g., X) to denote a map and small letter in bold (e.g., x_i) to denote its pixel-wise vector. We use upperscript s (*resp.*, u) to indicate seen (*resp.*, unseen) categories.

3.2 Contextual Module

Multi-scale Context Maps: We insert our Contextual Module (CM) after the backbone E of Deeplabv2, as shown in Figure 2. For the n -th image, we use $F_n \in \mathcal{R}^{h \times w \times l}$ to denote the output feature map of the E . Our CM aims to gather the pixel-wise contextual information for each pixel on F_n . Recall that the pixel-wise contextual information of a pixel means the aggregated information of its surrounding pixels. To achieve this goal, CM takes F_n as input to produce one or more context maps of the same size as F_n . Each

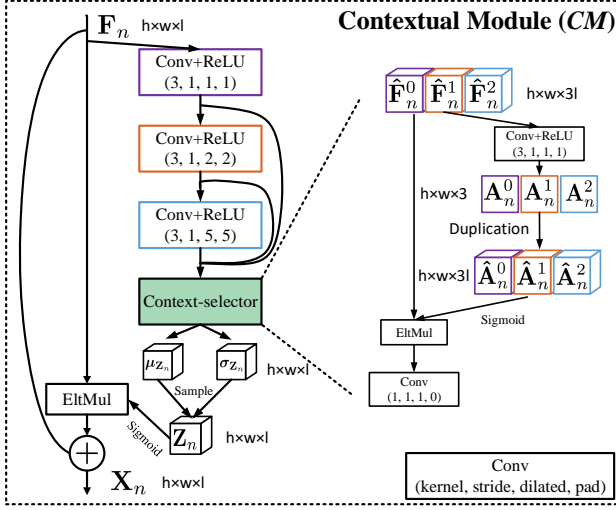


Figure 3: Contextual Module. We aggregate the contextual information of different scales using our context selector. Then, the aggregated contextual information produces latent distribution for sampling contextual latent code.

pixel-wise vector on context maps contains the pixel-wise contextual information of its corresponding pixel on F_n . In terms of the detailed design of CM, we consider two principles: 1) multi-scale contexts should be preserved for better feature generation; 2) the one-to-one correspondence between contexts and pixels should be maintained as discussed in Section 1, which means that no pooling layers should be used. Based on these principles, we employ several dilated conv layers [48] because they support the exponential expansion of receptive fields without loss of spatial resolution.

As shown in Figure 3, we use three serial dilated convs and refer to the output context maps of these layers as $\hat{F}_n^0, \hat{F}_n^1, \hat{F}_n^2 \in \mathcal{R}^{h \times w \times l}$ respectively. Applying three successive context maps can capture contextual information of different scales because pixels on a deeper context map have larger receptive fields, which means information within larger neighborhoods can be collected for these pixels.

Context Selector: Next, we attempt to aggregate three context maps. Intuitively, the features of different pixels may be dominated by the contextual information of small receptive field (e.g., the posture or inner parts of its belonging object) or large receptive field (e.g., distant background objects). To better select the contextual information of suitable scale for each pixel, we propose a light-weight context selector to adaptively learn different scale weights for different pixels. Specifically, we employ a 3×3 conv layer to transform the concatenated $[\hat{F}_n^0, \hat{F}_n^1, \hat{F}_n^2]$ to a 3-channel scale weight map $A_n = [A_n^0, A_n^1, A_n^2] \in \mathcal{R}^{h \times w \times 3}$, in which the k -th channel A_n^k contains the weights of all pixels for the k -th scale. Then, we duplicate each channel A_n^k to l channels to get $\hat{A}_n^k \in \mathcal{R}^{h \times w \times l}$ and obtain the weighted concatenation of three context maps $[\hat{F}_n^0 \odot \hat{A}_n^0, \hat{F}_n^1 \odot \hat{A}_n^1, \hat{F}_n^2 \odot \hat{A}_n^2] \in \mathcal{R}^{h \times w \times 3l}$ with \odot being Hadamard product. In this way, we select contexts of different scales pixel-wisely. Although our contextual module looks similar

to channel attention [14, 23] or full attention [41], our motivation and technical details are intrinsically different from them.

Contextual Latent Code: To obtain contextual latent code, we apply a 1×1 conv layer to the weighted concatenation of context maps $[\hat{F}_n^0 \odot \hat{A}_n^0, \hat{F}_n^1 \odot \hat{A}_n^1, \hat{F}_n^2 \odot \hat{A}_n^2]$ to output $\mu_{Z_n} \in \mathcal{R}^{h \times w \times l}$ and $\sigma_{Z_n} \in \mathcal{R}^{h \times w \times l}$, in which $\mu_{Z_n,i}$ and $\sigma_{Z_n,i}$ represent for each pixel-wise vector respectively. Then, the contextual latent code $z_{n,i}$ for the i -th pixel can be sampled from Gaussian distribution $\mathcal{N}(\mu_{Z_n,i}, \sigma_{Z_n,i})$ by using $z_{n,i} = \mu_{Z_n,i} + \epsilon \sigma_{Z_n,i}$, with epsilon being a random scalar sampled from $\mathcal{N}(0, 1)$. To enable stochastic sampling during inference, we employ a KL-divergence loss to enforce $\mathcal{N}(\mu_{Z_n,i}, \sigma_{Z_n,i})$ to be close to unit Gaussian distribution $\mathcal{N}(0, 1)$:

$$\mathcal{L}_{KL} = \mathcal{D}_{KL}[\mathcal{N}(\mu_{Z_n,i}, \sigma_{Z_n,i}) || \mathcal{N}(0, 1)].$$

We assume that the pixel-wise contextual latent code encodes the contextual information of this pixel. For instance, given a pixel in a cat near a tree, its contextual latent code may encode its near local region in the cat, its relative location in the cat, the posture of the cat, background objects like the tree, etc.

Furthermore, we aggregate all $z_{n,i}$ for the n -th image into latent code map $Z_n \in \mathcal{R}^{h \times w \times l}$. Inspired by [13], we element-multiply Z_n to F_n after applying sigmoid activation (denoted as ϕ) as residual attention, that is, our CM outputs the new feature map $X_n = F_n + F_n \odot \phi(Z_n) \in \mathcal{R}^{h \times w \times l}$ as both the target of feature generation and the input of classifier C . In this way, CM can be jointly trained with segmentation network as a residual attention module. Note that CM could slightly enhance the output feature map (X_n v.s. F_n of segmentation network, see Section 4.4), but the main goal of CM is to facilitate feature generation.

3.3 Context-aware Feature Generator

In this section, we first introduce the feature generation pipeline for seen categories, because training images only have pixel-wise annotations of seen objects. Given an input image I_n , the backbone E , together with the Contextual Module CM, delivers real visual feature map X_n^s with pixel-wise feature $\mathbf{x}_{n,i}^s$ and contextual latent code map $Z_n \in \mathcal{R}^{h \times w \times l}$ with pixel-wise latent code $z_{n,i}$ as mentioned in Section 3.2. For the i -th pixel on X_n^s , we have the category label $c_{n,i}^s$, which can also be represented by a one-hot vector $\mathbf{y}_{n,i}^s$ from the segmentation label map Y_n^s . Note that Y_n^s is a down-sampled label map with the same spatial resolution as X_n^s , i.e., $Y_n^s \in \mathcal{R}^{h \times w \times (|C^s| + |C^u|)}$. We can obtain the corresponding semantic word embedding map $\mathbf{W}_n^s \in \mathcal{R}^{h \times w \times d}$ with pixel-wise category embedding $\mathbf{w}_{n,i}^s = \mathbf{w}_{c_{n,i}^s}^s$. To generate fake pixel-wise feature, Z_n is then concatenated with \mathbf{W}_n^s as the input of generator G , which can be written as $\tilde{\mathbf{x}}_{n,i}^s = G(z_{n,i}, \mathbf{w}_{n,i}^s)$ for each pixel-wise generation process. As discussed in Section 1, since category-specific $\mathbf{w}_{n,i}^s$ and adequate contextual information $z_{n,i}$ is passed to G to resolve the ambiguity of output, we expect G to reconstruct the pixel-wise feature $\mathbf{x}_{n,i}^s$. This goal is accomplished by a L2 reconstruction loss \mathcal{L}_{REC} :

$$\mathcal{L}_{REC} = \sum_{n,i} \|\mathbf{x}_{n,i}^s - \tilde{\mathbf{x}}_{n,i}^s\|_2^2. \quad (1)$$

We also use a classification loss and an adversarial loss to regulate the generated features. Since the down-sampled label map Y_n^s has

the same spatial resolution as the real feature map $\mathbf{X}_n^s, \mathbf{y}_{n,i}^s$ one-to-one corresponds to $\mathbf{x}_{n,i}^s$ pixel-wisely. Following many segmentation papers [5, 25, 26, 50], we use the cross-entropy loss function as classification loss \mathcal{L}_{CLS} . It can be written as

$$\mathcal{L}_{CLS} = - \sum_{n,i} \mathbf{y}_{n,i}^s \log(C(\mathbf{x}_{n,i}^s)), \quad (2)$$

where the segmentation score from C is normalized by a softmax function. Following [29], adversarial loss \mathcal{L}_{ADV} can be written as

$$\mathcal{L}_{ADV} = \sum_{n,i} (D(\mathbf{x}_{n,i}^s))^2 + (1 - D(G(\mathbf{z}_{n,i}, \mathbf{w}_{n,i}^s)))^2, \quad (3)$$

in which the discrimination score from D is normalized within $[0, 1]$ by a sigmoid function, with target 1 (*resp.*, 0) indicating real (*resp.*, fake) pixel-wise features.

Then, we introduce the pixel-wise feature generation pipeline for both seen and unseen categories. We can feed a latent code \mathbf{z} randomly sampled from $\mathcal{N}(0, 1)$ and a semantic word embedding $\tilde{\mathbf{w}}_c$ into G to generate a pixel-wise feature $G(\mathbf{z}, \tilde{\mathbf{w}}_c)$ for arbitrary category $c \in \mathcal{C}^s \cup \mathcal{C}^u$. Intuitively, $G(\mathbf{z}, \tilde{\mathbf{w}}_c)$ stands for the pixel-wise feature of category c in the context encoded by \mathbf{z} .

3.4 Optimization

As shown in Figure 2, our optimization procedure has two steps in different colors: training and finetuning.

1) **Training:** In this step, the segmentation network and the feature generation network are trained jointly based on image data and segmentation masks of only seen categories. All network modules (E, CM, G, D, C) are updated. The objective function contains the loss terms introduced in Section 3.3:

$$\min_{G, E, C, CM} \max_D \mathcal{L}_{CLS} + \mathcal{L}_{ADV} + \lambda_1 \mathcal{L}_{REC} + \lambda_2 \mathcal{L}_{KL}.$$

Note that during optimization, we first update the parameters in D by maximizing the objective function, aiming to improve the discrimination ability of D . Then we try to minimize the objective function to update the other parameters of the network to both enhance the performances of segmentation and feature generation.

2) **Finetuning:** In this step, we consider both seen and unseen categories, so that the segmentation network can generalize well to unseen categories. For ease of computation, we construct the m -th word embedding map $\tilde{\mathbf{W}}_m^{sUu} \in \mathcal{R}^{h \times w \times d}$ by randomly stacking pixel-wise word embeddings $\tilde{\mathbf{w}}_{m,i}^{sUu}$ of both seen and unseen categories. The corresponding label map is $\tilde{\mathbf{Y}}_m^{sUu}$ with pixel-wise label vector $\tilde{\mathbf{y}}_{m,i}^{sUu}$. We use approximately the same number of seen and unseen pixels in each $\tilde{\mathbf{W}}_m^{sUu}$, which can generally achieves good performances as discussed in Table 5 of Section 4.5. Then, we generate fake feature map $\tilde{\mathbf{X}}_m^{sUu}$ with pixel-wise feature $\tilde{\mathbf{x}}_{m,i}^{sUu}$, based on $\tilde{\mathbf{W}}_m^{sUu}$ and contextual latent code map $\tilde{\mathbf{Z}}_m$ with pixel-wise latent code $\tilde{\mathbf{z}}_{m,i}$ sampled from $\mathcal{N}(\mathbf{0}, \mathbf{1})$. The above pixel-wise feature generation process can be formulated as $\tilde{\mathbf{x}}_{m,i}^{sUu} = G(\tilde{\mathbf{z}}_{m,i}, \tilde{\mathbf{w}}_{m,i}^{sUu})$. We freeze E and CM because there are no real visual features for gradient backpropagation. Only G, D , and C are updated. Thus, the objective function can be written as

$$\min_{G, C} \max_D \tilde{\mathcal{L}}_{CLS} + \tilde{\mathcal{L}}_{ADV},$$

in which $\tilde{\mathcal{L}}_{CLS}$ is obtained by replacing $\mathbf{y}_{n,i}^s$ (*resp.*, $\mathbf{x}_{n,i}^s$) in (2) with $\tilde{\mathbf{y}}_{m,i}^{sUu}$ (*resp.*, $\tilde{\mathbf{x}}_{m,i}^{sUu}$). For $\tilde{\mathcal{L}}_{ADV}$, we replace $\mathbf{w}_{n,i}^s$ (*resp.*, $\mathbf{z}_{n,i}$) in (3) with $\tilde{\mathbf{w}}_{m,i}^{sUu}$ (*resp.*, $\tilde{\mathbf{z}}_{m,i}$), and delete the first term $(D(\mathbf{x}_{n,i}^s))^2$ within the summation formula since we have no real features in this step. The optimizing process is the same as the training step by iteratively maximizing and minimizing the objective function.

By using ResNet-101 [16] pre-trained on ImageNet [39] as the initialization of backbone E , we first apply the training step on our network for enough iterations. Next, we iteratively perform training and finetuning steps every 100 iterations to balance the network optimization based on real features and fake features. In the testing stage, a test image goes through segmentation backbone E and Contextual Module CM to obtain its real visual feature map, which is passed to classifier C to achieve segmentation results.

4 EXPERIMENTS

4.1 Datasets and Semantic Embeddings

We evaluate our model on three benchmark datasets: Pascal-Context [31], COCO-stuff [4], and Pascal-VOC 2012 [6]. The Pascal-Context dataset contains 4998 training and 5105 validation images of 33 object/stuff categories. COCO-stuff has 164K images with dense pixel-wise annotations from 182 categories. Pascal-VOC 2012 contains 1464 training images with segmentation annotations of 20 object categories. For Pascal-VOC, following ZS3Net and SPNet, we adopt additional supervision from semantic boundary annotations [12] during training.

The experiment settings of two previous works, *i.e.*, SPNet and ZS3Net, are different in many aspects (*e.g.*, dataset, seen/unseen category split, backbone, semantic word embedding, evaluation metrics). SPNet reports results on large-scale COCO-stuff dataset [4], which makes their results more convincing. Besides, ZS3Net uses the word embedding of “background” as the semantic representation of all categories (*e.g.*, sky and ground) belonging to “background”, which seems a little unreasonable, while SPNet ignores “background” in both training and validation. Thus, we choose to strictly follow the settings of SPNet. But we also report the results by strictly following the settings of ZS3Net in the supplementary.

Following SPNet [43], we concatenate two different types of word embeddings ($d = 600, 300$ for each), *i.e.*, word2vec [30] trained on Google News and fast-Text [15] trained on Common Crawl. The word embeddings of categories that contain multiple words are obtained by averaging the embeddings of each individual word.

Our training/test sets are based on the standard train/test splits of three datasets, but we only use the pixel-wise annotations of seen categories and ignore the unseen pixels during training. For seen/unseen category split, following SPNet, we treat “frisbee, skateboard, cardboard, carrot, scissors, suitcase, giraffe, cow, road, wall-concrete, tree, grass, river, clouds, playingfield” as 15 unseen categories on COCO-stuff, and treat “potted plant, sheep, sofa, train, tv monitor” as 5 unseen categories on Pascal-VOC. We additionally report results on Pascal-Context with 33 categories, which is a popular segmentation dataset but not used in [43]. On Pascal-Context, we treat “cow, motorbike, sofa, cat” as 4 unseen categories.

Pascal-Context										
Method	Overall				Seen			Unseen		
	hIoU	mIoU	pixel acc.	mean acc.	mIoU	pixel acc.	mean acc.	mIoU	pixel acc.	mean acc.
SPNet	0	0.2938	0.5793	0.4486	0.3357	0.6389	0.5105	0	0	0
SPNet-c	0.0718	0.3079	0.5790	0.4488	0.3514	0.6213	0.4915	0.0400	0.1673	0.1361
ZS3Net	0.1246	0.3010	0.5710	0.4442	0.3304	0.6099	0.4843	0.0768	0.1922	0.1532
CaGNet	0.2061	0.3347	0.5924	0.4900	0.3610	0.6189	0.5140	0.1442	0.3341	0.3161
ZS3Net+ST	0.1488	0.3102	0.5725	0.4532	0.3398	0.6107	0.4935	0.0953	0.2030	0.1721
CaGNet+ST	0.2252	0.3352	0.5961	0.4962	0.3644	0.6120	0.5065	0.1630	0.4038	0.4214

COCO-stuff										
SPNet	0.0140	0.3164	0.5132	0.4593	0.3461	0.6564	0.5030	0.0070	0.0171	0.0007
SPNet-c	0.1398	0.3278	0.5341	0.4363	0.3518	0.6176	0.4628	0.0873	0.2450	0.1614
ZS3Net	0.1495	0.3328	0.5467	0.4837	0.3466	0.6434	0.5037	0.0953	0.2275	0.2701
CaGNet	0.1819	0.3345	0.5658	0.4845	0.3549	0.6562	0.5066	0.1223	0.2545	0.2701
ZS3Net+ST	0.1620	0.3367	0.5631	0.4862	0.3489	0.6584	0.5042	0.1055	0.2488	0.2718
CaGNet+ST	0.1946	0.3372	0.5676	0.4854	0.3555	0.6587	0.5058	0.1340	0.2670	0.2728

Pascal-VOC										
SPNet	0.0002	0.5687	0.7685	0.7093	0.7583	0.9482	0.9458	0.0001	0.0007	0.0001
SPNet-c	0.2610	0.6315	0.7755	0.7188	0.7800	0.8877	0.8791	0.1563	0.2955	0.2387
ZS3Net	0.2874	0.6164	0.7941	0.7349	0.7730	0.9296	0.8772	0.1765	0.2147	0.1580
CaGNet	0.3972	0.6545	0.8068	0.7636	0.7840	0.8950	0.8868	0.2659	0.4297	0.3940
ZS3Net+ST	0.3328	0.6302	0.8095	0.7382	0.7802	0.9189	0.8569	0.2115	0.3407	0.2637
CaGNet+ST	0.4366	0.6577	0.8164	0.7560	0.7859	0.8704	0.8390	0.3031	0.5855	0.5071

Table 1: Zero-shot segmentation performances on Pascal-Context, COCO-stuff and Pascal-VOC. “ST” stands for self-training. The best results with or w/o self-training are denoted in boldface, respectively.

4.2 Implementation Details

Our generator G is a multi-layer perceptron (512 hidden neurons, Leaky ReLU and dropout for each layer). Our classifier C and discriminator D consist of two 1×1 conv layers and share the same weights in the first conv layer. During training, the learning rate is initialized as $2.5e^{-4}$ and divided by 10 when the loss stops decreasing. The size of the training batch is 8 on one Tesla V100. All input images are 368 in size. We set $\lambda_1 = 10$, $\lambda_2 = 100$ via cross-validation by splitting a set of validation categories from seen categories. The analyses of λ_1, λ_2 can be found in the supplementary. We report results based on three evaluation metrics, *i.e.*, pixel accuracy, mean accuracy and mean Intersection over Union (mIoU) for both seen and unseen categories. Moreover, we also calculate the harmonic IoU (hIoU) [43] of all categories.

4.3 Comparison with State-of-the-art

We compare our method with two baselines: SPNet [43] and ZS3Net [3]. For a fair comparison, we use the same backbone Deeplabv2 as in [43] for all methods. We also report the results of SPNet-c which deducts the prediction scores of seen categories by a calibration factor. Besides, we additionally employ the Self-Training (ST) strategy in [3] for both ZS3Net and our method. Specifically, we tag unlabeled pixels in training images using the trained segmentation model and add them to the training set to finetune the segmentation model iteratively. We do not compare with ZS3Net (GC) in [3], because their used graph contexts are unavailable in our setting and also difficult to acquire in real-world applications.

Among evaluation metrics, “IoU” quantizes the overlap between predicted and ground-truth objects, which is more reliable than “accuracy” considering the integrity of objects. For “overall” evaluation, “hIoU” is more valuable than “mIoU”, because seen categories often have much higher mIoUs and dominate overall results.

Experimental results are summarized in Table 1. For unseen and overall evaluation, our CaGNet achieves significant improvement over SPNet¹ and ZS3Net on all three datasets, especially *w.r.t.* “mIoU” and “hIoU”. For seen evaluation, our method underperforms SPNet in some cases, because SPNet almost segments all pixels as seen categories while our method sacrifices some seen pixels for much better unseen performance.

4.4 Ablation Study

We evaluate our CaGNet on Pascal-VOC for ablation studies. We only report four reliable evaluation metrics: hIoU, mIoU, seen IoU (S-mIoU), and unseen IoU (U-mIoU), as claimed in Section 4.3.

Validation of network modules: We validate the effectiveness of each module (E, C, G, D, CM) in our method. The results are reported in Table 2, from which we can see that simply applying CM to the segmentation network only brings marginal improvement. Feature generation with G, D significantly raises the performance of unseen categories due to the reduced gap between seen and unseen categories. Finally, our proposed Contextual Module (CM) achieves evident improvements *w.r.t.* all metrics.

¹Our reproduced results of SPNet on Pascal-VOC dataset are obtained using their released model and code with careful tuning, but still lower than their reported results.

$E \& C$	G	D	CM	hIoU	mIoU	S-mIoU	U-mIoU
✓				0	0.5687	0.7583	0
✓			✓	0	0.5689	0.7599	0
✓	✓			0.2911	0.6332	0.7633	0.1798
✓	✓	✓		0.3105	0.6387	0.7751	0.1941
✓	✓	✓	✓	0.3972	0.6545	0.7840	0.2659

Table 2: Ablation studies of different network modules on Pascal-VOC. S-mIoU (*resp.*, U-mIoU) is the mIoU of seen (*resp.*, unseen) categories.

Layer	Dilated	MS	CS	hIoU	mIoU	S-mIoU	U-mIoU
conv (1×1)				0.3211	0.6394	0.7762	0.2023
conv				0.3298	0.6408	0.7768	0.2093
conv	✓			0.3654	0.6502	0.7789	0.2386
conv	✓	✓		0.3825	0.6526	0.7810	0.2532
conv (mask)	✓	✓	✓	0.3961	0.6538	0.7821	0.2652
conv	✓	✓	○	0.3902	0.6529	0.7816	0.2600
conv	✓	✓	✓	0.3972	0.6545	0.7840	0.2659

Table 3: Ablation studies of different variants of the contextual module on Pascal-VOC. “MS” and “CS” stand for Multi-Scale and Context Selector respectively.

loss	hIoU	mIoU	S-mIoU	U-mIoU
w/o \mathcal{L}_{KL}	0.3772	0.6513	0.7801	0.2487
w/o \mathcal{L}_{GAN}	0.3154	0.6392	0.7753	0.1979
w/o \mathcal{L}_{REC}	0.2176	0.6473	0.7835	0.1263
CaGNet	0.3972	0.6545	0.7840	0.2659

Table 4: Ablation studies of loss terms on Pascal-VOC.

Variants of contextual module: We explore different architectures before predicting μ_{z_n} and σ_{z_n} in our Contextual Module (CM) from simple to complex in Table 3, in which the last row is our proposed CM. The first row simply utilizes two 1×1 conv layers without capturing contextual information, and the bad performance shows the benefit of using contextual information.

The second row utilizes five standard conv layers (number of model parameters equal to our CM) to capture contextual information. The third row replaces the first three conv layers in the second row with three dilated conv layers as in our CM and achieves better results, which shows the benefit of using dilated conv. Built upon the third row, the fourth row further concatenates multi-scale contextual information $[\hat{F}_n^0, \hat{F}_n^1, \hat{F}_n^2]$ as in our CM and applies a 1×1 conv layer, but does not use the context selector. The fourth row is better than the third row but worse than the last row, which proves the advantage of aggregating multi-scale contextual information and adaptively weighting different scales for different pixels.

We also study a special case of our CM in the fifth row named “conv (mask)”. The only difference is that we set the central $1 \times 1 \times l$ weights of all $3 \times 3 \times l$ conv filters as constant zeros without any update in the first dilated conv layer. In this way, when gathering the contextual information for each pixel, we roughly eliminate the

r (seen:unseen)	hIoU	mIoU	S-mIoU	U-mIoU
$ C^s : C^u $	0.2887	0.6425	0.7898	0.1763
1 : 1	0.3972	0.6545	0.7840	0.2659
1 : 10	0.3896	0.6375	0.7687	0.2617
0 : 1	0.3766	0.6024	0.6620	0.2632

Table 5: Performances of different feature generating ratio r during the finetuning step on Pascal-VOC.

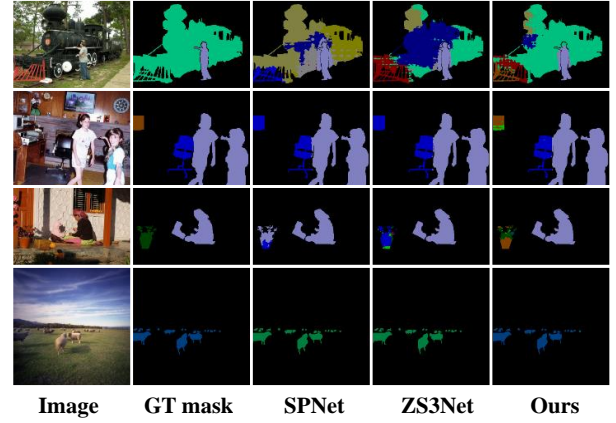


Figure 4: Visualization of zero-shot segmentation results on Pascal-VOC. GT mask is ground-truth segmentation mask.

impact of its own pixel-wise feature. The results in the fifth row are comparable with those in the last row, so it does not matter whether to eliminate the pixel-wise information for each pixel themselves.

Another variant of our CM is in the sixth row, in which ○ means we modify the context selector by learning only one weight for each scale without considering inter-pixel difference. Specifically, we perform global average pooling on $[\hat{F}_n^0, \hat{F}_n^1, \hat{F}_n^2]$ followed by a FC to obtain a $1 \times 1 \times 3$ scale weight vector, which is replicated to an $h \times w \times 3l$ scale weight map. The results in the sixth row are also worse than the last row, showing the effectiveness of contextual information. Besides these results, we also evaluate two more special cases of CM, “w/o residual” and “Parallel” in the supplementary.

Validation of loss terms: We remove each loss term (*i.e.*, \mathcal{L}_{KL} , \mathcal{L}_{ADV} , \mathcal{L}_{REC}) and report the results in Table 4. We observe that the performance becomes worse after removing any loss, which demonstrates that all loss terms contribute to better performance.

4.5 Hyper-parameter Analysis

There exists a hyper-parameter during the finetuning step. We name it as the feature generating ratio (notated as r), which is the expected count ratio of seen pixels to unseen pixels while constructing each semantic word embedding map for feature generation. For example, if we randomly construct a word embedding map without any constraint, then $r = |C^s| : |C^u|$. However, in this case, seen features are much more than unseen features in pixel level (29:4 on Pascal-Context, 167:15 on COCO-stuff), leading to bad performances on unseen categories. After a few trials, we find that the

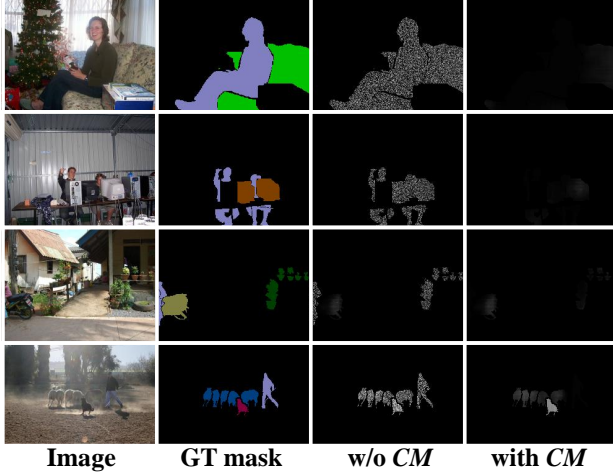


Figure 5: Visualization of context-aware feature generation on Pascal-VOC test set. GT mask is ground-truth segmentation mask. In the third and fourth columns, we show the reconstruction loss maps calculated based on the generated feature maps and real feature maps (the darker, the better).

reasonable feature generating ratio r is 1 : 1, as shown in Table 5. The analyses of the other two hyper-parameters λ_1, λ_2 can be found in the supplementary.

4.6 Qualitative Analyses

We also provide some visualizations on Pascal-VOC. More visualization results can be found in the Supplementary.

Semantic segmentation: We show the segmentation results of baselines and our method in Figure 4, in which “GT” means ground-truth. Our method performs more favorably when segmenting unseen objects, *e.g.*, the train (green), tv monitor (orange), potted plant (green), sheep (dark blue) in the sorted four rows.

Feature generation: To confirm the effectiveness of feature generation with Contextual Module (CM), we evaluate the generated features on test images. On the one hand, we feed ground-truth semantic word embeddings and latent code into the generator to obtain the generated feature map. On the other hand, we input the test image to the segmentation backbone to obtain the real feature map. Then, we show the reconstruction loss map calculated based on the generated and real feature maps in Figure 5, in which smaller loss implies better generation quality. We compare our method “with CM” (latent code is contextual latent code produced by CM) with the special case “w/o CM” (latent code is random vector). We can observe that our CM not only helps generate better features for seen categories (*e.g.*, “person”), but also for unseen categories (*e.g.*, “potted plant, sheep, sofa, tv monitor”).

Context selector: The target of our context selector is to select context of the suitable scale for each pixel based on the scale weight map $[\mathbf{A}_n^0, \mathbf{A}_n^1, \mathbf{A}_n^2] \in \mathcal{R}^{h \times w \times 3}$, in which each pixel-wise vector contains three scale weights for the pixel it corresponds to. In our implementation, \mathbf{A}_n^0 (*resp.*, $\mathbf{A}_n^1, \mathbf{A}_n^2$) corresponds to small scale (*resp.*, middle scale, large scale) with the size of receptive field being 3×3

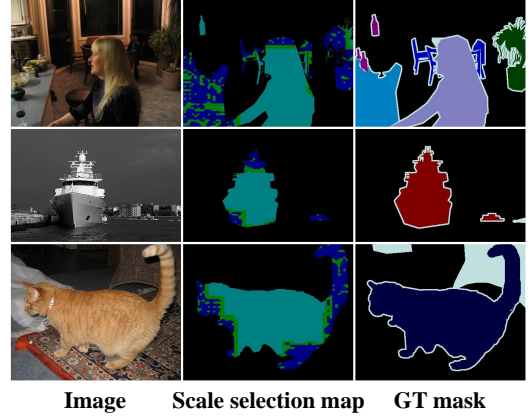


Figure 6: Visualization of the effectiveness of context selector on Pascal-VOC. GT mask is ground-truth segmentation mask. The scale selection map is obtained from the scale weight map, in which dark blue, green, light blue represents small scale, middle scale, and large scale respectively.

(*resp.*, $7 \times 7, 17 \times 17$) w.r.t. the input feature map \mathbf{F}_n . In Figure 6, we list some examples with their corresponding scale selection maps and ground-truth segmentation masks. Note that the scale selection map is obtained from the scale weight map by choosing the scale with the largest weight for each pixel. We use three colors to indicate the most suitable scale (largest weight) of each pixel. In detail, dark blue, green, and light blue represent small scale, medium scale, and large scale respectively. From Figure 6, we can observe that the pixels within discriminative local regions prefer the small scale while the other pixels prefer medium or large scale, which can be explained as follows. For the pixels within discriminative local regions (*e.g.*, animal faces, small objects on the table), small-scale contextual information is sufficient for reconstructing pixel-wise features, while other pixels may require contextual information of larger scale. Another observation is small (*resp.*, large) objects prefer small (*resp.*, large) scale (*e.g.*, the small boat and the large boat in the second row). These observations verify our motivation and the effectiveness of our proposed context selector.

5 CONCLUSION

In this work, we have unified the segmentation network and feature generation for zero-shot semantic segmentation, which utilizes contextual information to generate diverse and context-aware features. Qualitative and quantitative results on three benchmark datasets have shown the effectiveness of our method.

ACKNOWLEDGMENTS

The work is supported by the National Key R&D Program of China (2018AAA0100704) and is partially sponsored by the National Natural Science Foundation of China (Grant No.61902247) and Shanghai Sailing Program (19YF1424400).

REFERENCES

- [1] Zeynep Akata, Florent Perronnin, Zaid Harchaoui, and Cordelia Schmid. 2015. Label-Embedding For Image Classification. *TPAMI* 38, 7 (2015), 1425–1438.
- [2] Zeynep Akata, Scott Reed, Daniel Walter, Honglak Lee, and Bernt Schiele. 2015. Evaluation Of Output Embeddings For Fine-Grained Image Classification. In *CVPR*.
- [3] Maxime Bucher, Tuan-Hung Vu, Mathieu Cord, and Patrick Pérez. 2019. Zero-Shot Semantic Segmentation. In *NeurIPS*.
- [4] Holger Caesar, Jasper Uijlings, and Vittorio Ferrari. 2018. Coco-Stuff: Thing And Stuff Classes In Context. In *CVPR*.
- [5] Liang-Chieh Chen, George Papandreou, Iasonas Kokkinos, Kevin Murphy, and Alan L Yuille. 2018. Deeplab: Semantic Image Segmentation With Deep Convolutional Nets, Atrous Convolution, And Fully Connected CRFs. *TPAMI* 40, 4 (2018), 834–848.
- [6] Mark Everingham, S. M. Ali Eslami, Luc Van Gool, Christopher K. I. Williams, John Winn, and Andrew Zisserman. 2015. ThePascalVisual Object Classes Challenge: A Retrospective. *IJCV* 111, 1 (2015), 98–136.
- [7] Rafael Felix, B. G. Vijay Kumar, Ian Reid, and Gustavo Carneiro. 2018. Multi-Modal Cycle-Consistent Generalized Zero-Shot Learning. In *ECCV*.
- [8] Andrea Frome, Greg S Corrado, Jon Shlens, Samy Bengio, Jeff Dean, Marc’Aurelio Ranzato, and Tomas Mikolov. 2013. Devise: A Deep Visual-Semantic Embedding Model. In *NeurIPS*.
- [9] Yanwei Fu, Timothy M Hospedales, Tao Xiang, and Shaogang Gong. 2015. Transductive Multi-View Zero-Shot Learning. *TPAMI* 37, 11 (2015), 2332–2345.
- [10] Yuchen Guo, Guiguang Ding, Jungong Han, Hang Shao, Xin Lou, and Qionghai Dai. 2019. Zero-Shot Learning With Many Classes By High-Rank Deep Embedding Networks. In *IJCAI*.
- [11] Amirhossein Habibi, Thomas Mensink, and Cees G. M. Snoek. 2014. Composite Concept Discovery For Zero-Shot Video Event Detection. In *ACMMM*.
- [12] Bharath Hariharan, Pablo Arbelaez, Lubomir D. Bourdev, Subhansu Maji, and Jitendra Malik. 2011. Semantic Contours From Inverse Detectors. In *ICCV*.
- [13] Jie Hu, Li Shen, Samuel Albanie, Gang Sun, and Andrea Vedaldi. 2018. Gather-Excite: Exploiting Feature Context In Convolutional Neural Networks. In *NeurIPS*.
- [14] Gang Sun, Jie Hu, Li Shen. 2018. Squeeze-And-Excitation Networks. In *CVPR*.
- [15] Armand Joulin, Edouard Grave, Piotr Bojanowski, and Tomas Mikolov. 2017. Bag Of Tricks For Efficient Text Classification. In *ECAL*.
- [16] Shaoqing Ren, Kaiming He, Xiangyu Zhang and Jian Sun. 2016. Deep Residual Learning For Image Recognition. In *CVPR*.
- [17] Naoki Kato, Toshihiko Yamasaki, and Kiyoharu Aizawa. 2019. Zero-Shot Semantic Segmentation Via Variational Mapping. In *ICCV Workshops*.
- [18] Anna Khoreva, Rodrigo Benenson, Jan Hosang, Matthias Hein, and Bernt Schiele. 2017. Simple Does It: Weakly Supervised Instance And Semantic Segmentation. In *CVPR*.
- [19] Thomas Kipf and Max Welling. 2017. Semi-Supervised Classification With Graph Convolutional Networks. *ICLR*.
- [20] Christoph H. Lampert, Hannes Nickisch, and Stefan Harmeling. 2009. Learning To Detect Unseen Object Classes By Between-Class Attribute Transfer. In *CVPR*.
- [21] Christoph H Lampert, Hannes Nickisch, and Stefan Harmeling. 2013. Attribute-Based Classification For Zero-Shot Visual Object Categorization. *TPAMI* 36, 3 (2013), 453–465.
- [22] Jingjing Li, Mengmeng Jin, Ke Lu, Zhengming Ding, Lei Zhu, and Zi Huang. 2019. Leveraging The Invariant Side Of Generative Zero-Shot Learning. In *CVPR*.
- [23] Wei Li, Xiatian Zhu, and Shaogang Gong. 2018. Harmonious Attention Network For Person Re-Identification. In *CVPR*.
- [24] Di Lin, Jifeng Dai, Jiaya Jia, Kaiming He, and Jian Sun. 2016. Scribblesup: Scribble-Supervised Convolutional Networks For Semantic Segmentation. In *CVPR*.
- [25] Guosheng Lin, Anton Milan, Chunhua Shen, and Ian Reid. 2017. RefineNet: Multi-Path Refinement Networks For High-Resolution Semantic Segmentation. In *CVPR*.
- [26] Jonathan Long, Evan Shelhamer, and Trevor Darrell. 2015. Fully Convolutional Networks For Semantic Segmentation. In *CVPR*.
- [27] Teng Long, Xing Xu, Youyou Li, Fumin Shen, Jingkuan Song, and Heng Tao Shen. 2018. Pseudo Transfer With Marginalized Corrupted Attribute For Zero-Shot Learning. In *ACMMM*.
- [28] Devraj Mandal, Sanath Narayan, Saikumar Dwivedi, Vikram Gupta, Shuaib Ahmed, Fahad Shahbaz Khan, and Ling Shao. 2019. Out-Of-Distribution Detection For Generalized Zero-Shot Action Recognition. In *CVPR*.
- [29] Xudong Mao, Qing Li, Haoran Xie, Raymond Y. K. Lau, Zhen Wang, and Stephen Paul Smolley. 2017. Least Squares Generative Adversarial Networks. In *ICCV*.
- [30] Tomas Mikolov, Ilya Sutskever, Kai Chen, Greg S Corrado, and Jeff Dean. 2013. Distributed Representations Of Words And Phrases And Their Compositionality. In *NeurIPS*.
- [31] Roozbeh Mottaghi, Xianjie Chen, Xiaobai Liu, Nam-Gyu Cho, Seong-Whan Lee, Sanja Fidler, Raquel Urtasun, and Alan Yuille. 2014. The Role Of Context For Object Detection And Semantic Segmentation In The Wild. In *CVPR*.
- [32] Li Niu, Jianfei Cai, Ashok Veeraraghavan, and Liqing Zhang. 2019. Zero-Shot Learning via Category-Specific Visual-Semantic Mapping and Label Refinement. *IEEE Transactions on Image Processing* 28, 2 (2019), 965–979.
- [33] Li Niu, Ashok Veeraraghavan, and Ashu Sabharwal. 2018. Webly Supervised Learning Meets Zero-shot Learning: A Hybrid Approach for Fine-Grained Classification. In *CVPR*.
- [34] Seong Joon Oh, Rodrigo Benenson, Anna Khoreva, Zeynep Akata, Mario Fritz, and Bernt Schiele. 2017. Exploiting Saliency For Object Segmentation From Image Level Labels. In *CVPR*.
- [35] George Papandreou, Liang-Chieh Chen, Kevin P Murphy, and Alan L Yuille. 2015. Weakly-And Semi-Supervised Learning Of A Deep Convolutional Network For Semantic Image Segmentation. In *ICCV*.
- [36] Mengyang Pu, Yaping Huang, Qingji Guan, and Qi Zou. 2018. GraphNet: Learning Image Pseudo Annotations For Weakly-Supervised Semantic Segmentation. In *ACMMM*.
- [37] Bernardino Romera-Paredes and Philip Torr. 2015. An Embarrassingly Simple Approach To Zero-Shot Learning. In *ICML*.
- [38] Olaf Ronneberger, Philipp Fischer, and Thomas Brox. 2015. U-Net: Convolutional Networks For Biomedical Image Segmentation. In *MICCAI*.
- [39] Olga Russakovsky, Jia Deng, Hao Su, Jonathan Krause, Sanjeev Satheesh, Sean Ma, Zhiheng Huang, Andrej Karpathy, Aditya Khosla, Michael Bernstein, Alexander C. Berg, and Li Fei-Fei. 2015. ImageNet Large Scale Visual Recognition Challenge. *IJCV* 115, 3 (2015), 211–252.
- [40] Mert Bulent Sariyildiz and Ramazan Gokberk Cinbis. 2019. Gradient Matching Generative Networks For Zero-Shot Learning. In *CVPR*.
- [41] Cheng Wang, Qian Zhang, Chang Huang, Wenyu Liu, and Xinggang Wang. 2018. Mancs: A Multi-Task Attentional Network With Curriculum Sampling For Person Re-Identification. In *ECCV*.
- [42] Wenqi Xian, Patson Sangkloy, Varun Agrawal, Amit Raj, Jingwan Lu, Chen Fang, Fisher Yu, and James Hays. 2018. Texturegan: Controlling Deep Image Synthesis With Texture Patches. In *CVPR*.
- [43] Yongqin Xian, Subhabrata Choudhury, Yang He, Bernt Schiele, and Zeynep Akata. 2019. Semantic Projection Network For Zero-and Few-Label Semantic Segmentation. In *CVPR*.
- [44] Yongqin Xian, Tobias Lorenz, Bernt Schiele, and Zeynep Akata. 2018. Feature Generating Networks For Zero-Shot Learning. In *CVPR*.
- [45] Yongqin Xian, Saurabh Sharma, Bernt Schiele, and Zeynep Akata. 2019. f-VAEGAN-D2: A Feature Generating Framework For Any-Shot Learning. In *CVPR*.
- [46] Yang Yang, Yadan Luo, Weilun Chen, Fumin Shen, Jie Shao, and Heng Tao Shen. 2016. Zero-Shot Hashing Via Transferring Supervised Knowledge. In *ACMMM*.
- [47] Xiwen Yao, Junwei Han, Cheng Gong, and Guo Lei. 2015. Semantic Segmentation Based On Stacked Discriminative Autoencoders And Context-Constrained Weakly Supervised Learning. In *ACMMM*.
- [48] Fisher Yu and Vladlen Koltun. 2016. Multi-Scale Context Aggregation By Dilated Convolutions. In *ICLR*.
- [49] Hang Zhao, Xavier Puig, Bolei Zhou, Sanja Fidler, and Antonio Torralba. 2017. Open Vocabulary Scene Parsing. In *ICCV*.
- [50] Hengshuang Zhao, Jianping Shi, Xiaojuan Qi, Xiaogang Wang, and Jiaya Jia. 2017. Pyramid Scene Parsing Network. In *CVPR*.
- [51] Jun-Yan Zhu, Taesung Park, Phillip Isola, and Alexei A Efros. 2017. Unpaired Image-To-Image Translation Using Cycle-Consistent Adversarial Networks. In *ICCV*.
- [52] Jun-Yan Zhu, Richard Zhang, Deepak Pathak, Trevor Darrell, Alexei A Efros, Oliver Wang, and Eli Shechtman. 2017. Toward Multimodal Image-To-Image Translation. In *NeurIPS*.
- [53] Ling Xie Jingyi Yu Shenghua Gao Ziheng Zhang, Anpei Chen. 2019. Learning Semantics-Aware Distance Map With Semantics Layering Network For Amodal Instance Segmentation. In *ACMMM*.

Supplementary for Context-aware Feature Generation For Zero-shot Semantic Segmentation

Zhangxuan Gu Siyuan Zhou Li Niu*
 MoE Key Lab of Artificial Intelligence, MoE Key Lab of Artificial Intelligence, MoE Key Lab of Artificial Intelligence,
 Shanghai Jiao Tong University Shanghai Jiao Tong University Shanghai Jiao Tong University
 zhangxgu@126.com ssluvble@sjtu.edu.cn ustcnewly@sjtu.edu.cn

Zihan Zhao Liqing Zhang*
 MoE Key Lab of Artificial Intelligence, MoE Key Lab of Artificial Intelligence,
 Shanghai Jiao Tong University Shanghai Jiao Tong University
 john745111625@gmail.com zhang-lq@cs.sjtu.edu.cn

CCS CONCEPTS

• **Computing methodologies** → **Image segmentation.**

ACM Reference Format:

Zhangxuan Gu, Siyuan Zhou, Li Niu*, Zihan Zhao, and Liqing Zhang*. 2020. Supplementary for Context-aware Feature Generation For Zero-shot Semantic Segmentation. In *Proceedings of the 28th ACM International Conference on Multimedia (MM '20)*, October 12–16, 2020, Seattle, WA, USA. ACM, New York, NY, USA, 3 pages. <https://doi.org/10.1145/3394171.3413593>

1 COMPARISON IN THE SETTING OF ZS3NET

To further verify the effectiveness of our proposed method, we also evaluate our method in the setting of ZS3Net [1] (*i.e.*, backbone, semantic word embedding method, seen/unseen splits, evaluation metrics). Note that we only follow the setting of ZS3Net [1] in this section, while in other sections we still follow SPNet [4].

Following ZS3Net [1], we use word2vec [3] embeddings in length 300 as semantic word embeddings and use deeplabv3+ [2] as the backbone. For both evaluation and training, we treat “background” as a seen category following ZS3Net. We conduct experiments on Pascal-VOC dataset with 20 categories and Pascal-Context dataset with 59 categories. For seen/unseen split, we choose one of the splits provided by ZS3Net for each dataset: “cow, motorbike, airplane, sofa” as 4 unseen categories on Pascal-VOC dataset, and “cow, motorbike, sofa, cat, boat, fence, bird, tvmonitor, keyboard, aeroplane” as 10 unseen categories on Pascal-Context dataset.

The experimental results are shown in Table 1 and the results of ZS3Net are directly copied from their paper. Our method achieves comparable or better results on seen categories. More importantly, our method significantly improves the results on unseen categories. For overall hIoU, our method achieves the improvement of 13.0 and 4.9 on Pascal-VOC and Pascal-Context respectively. This indicates

that our method still beats ZS3Net in their setting with dramatic improvements. Another observation is that our method has much larger performance gain on Pascal-VOC than Pascal-Context, which may be due to the difficulty in segmenting more unseen categories.

2 MORE ABLATION STUDIES ON OUR CONTEXTUAL MODULE

In this section, we add two more special cases “w/o residual” and “Parallel” to supplement Table 3 of Section 4.4 in the main paper, as part of the ablation studies on different variants of our Contextual Module.

In the special case “w/o residual”, our Contextual Module (*CM*) outputs the contextual latent code without being linked back to the segmentation network, so that residual attention is not applied to feature map F_n to obtain enhanced feature map X_n . In this case, the contextual latent code is obtained in the same way, while the target of feature reconstruction becomes F_n instead of X_n . We also replace X_n with F_n in all loss functions. The results are shown in the first row of Table 2. We can observe that linking our *CM* to the segmentation network improves the performances on all metrics.

In the special case “Parallel”, we change the way of arranging three dilated conv layers in *CM* from serial to parallel. That is, we parallelly put three dilated conv layers (same parameters as those in original *CM* respectively) after the input feature map F_n and obtain context maps of different receptive fields. The receptive fields of three dilated convs are 3×3 , 5×5 , and 13×13 on F_n respectively, which are equal to or smaller than those (3×3 , 7×7 , and 17×17) in the serial mode. The experiment results of the second row in Table 2 indicates that the serial mode in the main paper is more superior than the parallel mode, probably due to the larger receptive fields of the obtained context maps.

3 HYPER-PARAMETER ANALYSES

By taking Pascal-VOC dataset as an example, we investigate the impact of hyper-parameters λ_1, λ_2 in our method (depicted in Section 3.4 in the main paper). We vary λ_1 (*resp.*, λ_2) within the range $[0.1, 1000]$ and report hIoU (%) results of our method in Figure 1. We observe that λ_1 has larger impact and the performance drops sharply when λ_1 is very small, which proves the necessity of feature reconstruction. Our method is robust when setting λ_1 (*resp.*, λ_2) in a reasonable range $[10, 100]$ (*resp.*, $[1, 1000]$).

*Corresponding authors.

Permission to make digital or hard copies of all or part of this work for personal or classroom use is granted without fee provided that copies are not made or distributed for profit or commercial advantage and that copies bear this notice and the full citation on the first page. Copyrights for components of this work owned by others than ACM must be honored. Abstracting with credit is permitted. To copy otherwise, or republish, to post on servers or to redistribute to lists, requires prior specific permission and/or a fee. Request permissions from [permissions@acm.org](https://permissions.acm.org).

MM '20, October 12–16, 2020, Seattle, WA, USA

© 2020 Association for Computing Machinery.

ACM ISBN 978-1-4503-7988-5/20/10...\$15.00

<https://doi.org/10.1145/3394171.3413593>

Pascal-Context										
Method	Overall				Seen			Unseen		
	hIoU	mIoU	pixel acc.	mean acc.	mIoU	pixel acc.	mean acc.	mIoU	pixel acc.	mean acc.
ZS3Net	16.3	19.5	54.6	27.1	20.7	53.9	23.8	13.5	59.6	43.8
CaGNet	21.2	23.2	56.6	36.8	24.8	55.2	35.7	18.5	66.8	49.8

Pascal-VOC										
ZS3Net	37.9	61.1	90.8	73.5	69.3	92.9	78.7	26.1	46.7	51.5
CaGNet	50.9	63.2	91.4	74.6	69.5	92.7	78.9	40.2	67.8	52.3

Table 1: Zero-shot segmentation performances on Pascal-Context and Pascal-VOC datasets in the setting of ZS3Net. The best results are denoted in boldface.

	hIoU	mIoU	S-mIoU	U-mIoU
w/o residual	0.3862	0.6480	0.7815	0.2564
Paralle	0.3821	0.6509	0.7832	0.2527
CaGNet	0.3972	0.6545	0.7840	0.2659

Table 2: Ablation studies of special cases of the contextual module on Pascal-VOC.

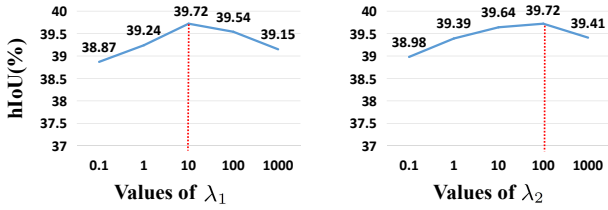


Figure 1: The effects of varying the values of λ_1, λ_2 on Pascal-VOC. The dashed lines denote the default values used in our paper.

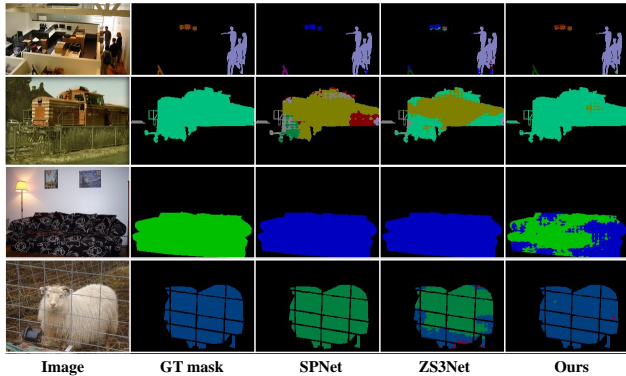


Figure 2: Visualization of segmentation results for different methods on Pascal-VOC dataset. GT mask is the ground-truth segmentation mask.

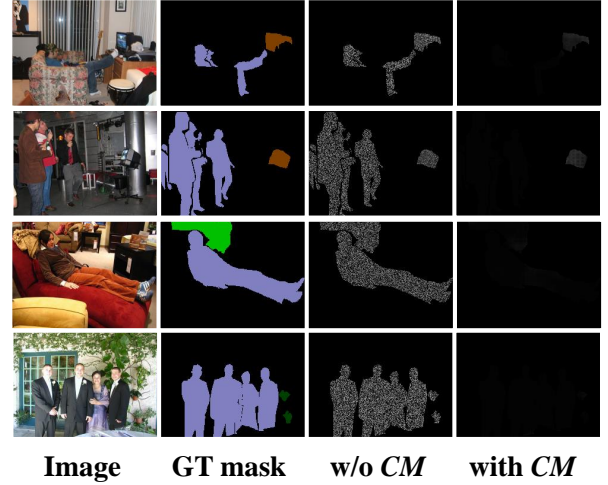


Figure 3: Visualization of the effectiveness of Contextual Module (CM) in feature generation on test images on Pascal-VOC dataset. In the second column, GT mask is the ground-truth segmentation mask. In the third and fourth columns, we show the reconstruction loss maps calculated based on the generated feature maps and real feature maps (the darker, the better).

4 MORE VISUALIZATIONS OF SEGMENTATION RESULTS

In this section, we show more visualizations of segmentation results for different methods in Figure 2, supplementing the visualizations in Figure 5 of Section 4.6 in the main paper.

As shown in Figure 2, our method beats others when segmenting unseen objects like “tv”, “train”, “sofa”, and “sheep”, which further proves the advantage of our method. For example, in the first and third row, SPNet and ZS3Net misclassify “tv” and “sofa” as “table”, but our method segments them successfully. We can also observe that “train” in the second row is hard to segment by SPNet and ZS3Net. This is probably because the word “train” contains several distinct meanings and only one of them represents the typical unseen category in the dataset. Therefore, the semantic word embedding of “train” is not accurate enough for the model to segment

objects of this category precisely. However, our method can still recognize and segment it. In the fourth row, “sheep” is also recognized by our method, while ZS3Net and SPNet classify it as “cow”.

5 MORE VISUALIZATIONS OF FEATURE GENERATION

We show more visualizations of feature generation in Figure 3, supplementing the visualizations in Figure 6 of Section 4.6 in the main paper. By taking test images of Pascal-VOC dataset as examples, we show the reconstruction loss maps calculated based on the generated feature maps and their according real feature maps, in which smaller loss (darker region) implies better generation quality. We compare the reconstruction loss maps obtained by using Contextual Module (*CM*) or without *CM*. It can be observed from Figure 3

that our *CM* not only facilitates generating better features for seen categories (e.g., “person”), but also for unseen categories (e.g., “tv” in brown in the first two rows, “potted plant” in dark green in the fourth row).

REFERENCES

- [1] Maxime Bucher, Tuan-Hung Vu, Mathieu Cord, and Patrick Pérez. 2019. Zero-Shot Semantic Segmentation. In *NeurIPS*.
- [2] George Papandreou Florian Schroff Hartwig Adam Liang-Chieh Chen, Yukun Zhu. 2018. Encoder-Decoder With Atrous Separable Convolution For Semantic Image Segmentation. In *ECCV*.
- [3] Tomas Mikolov, Ilya Sutskever, Kai Chen, Greg S Corrado, and Jeff Dean. 2013. Distributed Representations Of Words And Phrases And Their Compositionality. In *NeurIPS*.
- [4] Yongqin Xian, Subhabrata Choudhury, Yang He, Bernt Schiele, and Zeynep Akata. 2019. Semantic Projection Network For Zero-and Few-Label Semantic Segmentation. In *CVPR*.